Time-Modulated Antenna Array with Beam-Steering for Low-Power Wide-Area Network Receivers

Grzegorz Bogdan, *Member, IEEE*, Konrad Godziszewski, *Member, IEEE*, Yevhen Yashchyshyn, *Senior Member, IEEE*

***Abstract*— The Internet of Things (IoT) denotes a concept of connected devices that communicate seamlessly over the Internet. The wireless connectivity between IoT nodes and the Internet gateways can be realized in unlicensed frequency bands upon the low-power wide-area network (LPWAN). It is foreseen that due to a massive introduction of IoT devices the unlicensed bands will experience an increased interference level which will negatively affect the communication performance. Therefore, adaptive solutions should be considered to obtain robustness. This paper presents a time-modulated antenna array (TMAA) for LPWAN receivers and demonstrates its interoperability with a commercial of-the-shelf LoRa device. According to the conducted experimental investigation, whereby the beam-steering is obtained over the sidebands inherently generated by the TMAA, both the received signal strength and the signal-to-noise ratio are improved by means of the progressive delay applied to the time modulation functions.**

***Index Terms*—adaptive antennas, adaptive arrays, beam steering, time-modulated antenna arrays, interference suppression**

I. Introduction

THE Low-Power Wide-Area Network (LPWAN) is the key enabling technology for the Internet of Things (IoT) [1]. In Europe, LPWANs can be deployed in the unlicensed frequency band from 863 to 870 MHz [2]. The massive introduction of IoT devices and the use of unlicensed bands are greatly affecting the occupancy and thereby the interference levels [3]. Therefore, improved communication solutions must be implemented. For example, the chirp spread spectrum (CSS) modulation is utilized in the LoRa technology for LPWAN because of its robustness to narrow-band interferences [4], [5]. Immunity to unwanted signals can also be obtained by increasing the antenna gain in a desired direction and suppressing reception of interfering signals arriving from other directions. Such functionality can be provided to a wireless system by implementation of an adaptive antenna array (AAA); however, relatively high cost and high energy consumption of conventional AAAs are limiting their wide implementation in IoT devices [6].

In this letter we present AAA for IoT gateways based on a concept of the time-modulated antenna array (TMAA). This concept was selected due to its key advantages over conventional AAAs especially for IoT applications, i.e. low energy consumption and non-complex implementation [7]. TMAAs, despite their assets, possess one main drawback—limitation of a maximum signal bandwidth which can be processed without aliasing [8]. It can be extended with enhanced architectures [9] and advanced switching sequences [10], although, if the unwanted sidebands are not perfectly rejected they may cause an intrinsic interference when the signal bandwidth is larger than the time modulation frequency [11]. As a consequence, the applicability of TMAAs in modern wideband networks is restricted, because according to the current state-of-the-art the bandwidth of TMAAs is typically less than few megahertz when regular radio frequency (RF) switches are implemented [12]. Nevertheless, such a narrow bandwidth is sufficient for wireless networks based on LPWAN technology. Therefore, in this paper we present a TMAA designed for the LoRa receiver which is suitable for implementation in the receiving IoT gateways.

II. Theoretical Analysis

A. TMAA Array Factor

TMAAs are electromagnetic systems whose radiated power pattern is controlled by the application of variable-width and variable-duration periodic pulses to the individual elements [13]. The array factor of a linear TMAA composed of uniformly distributed elements can be formulated as:

$$AF(\theta,t) = e^{j2\pi f_c t}\sum_{n=0}^{N-1} I_n m_n(t) e^{j\beta n d\sin\theta} \qquad (1)$$

where θ is the angle in respect to the broadside direction, f_c is the carrier frequency, N is the number of elements in the array, I_n is the complex amplitude of an exciting signal applied to the nth element, $m_n(t)$ denotes the time modulation function applied to the nth element, d is the distance between elements of the array, $\beta = 2\pi/\lambda$ is the wavenumber in the free space, and λ is the wavelength in the free space. If $m_n(t)$ is periodic with the period

This work was supported by the Early Stage Researcher Grant program of Warsaw University of Technology, Faculty of Electronics and Information Technology (IRiTM/2019/dziek/2, Research on a Time-Modulated Antenna Array (TMAA) for Internet of Things (IoT) Wireless Networks)

G. Bogdan, K. Godziszewski, and Y. Yashchyshyn are with the Institute of Radioelectronics and Multimedia Technology, Warsaw University of Technology, Warsaw, Poland (e-mail: g.bogdan@ire.pw.edu.pl, k.godziszewski@ire.pw.edu.pl, y.yashchyshyn@ire.pw.edu.pl).

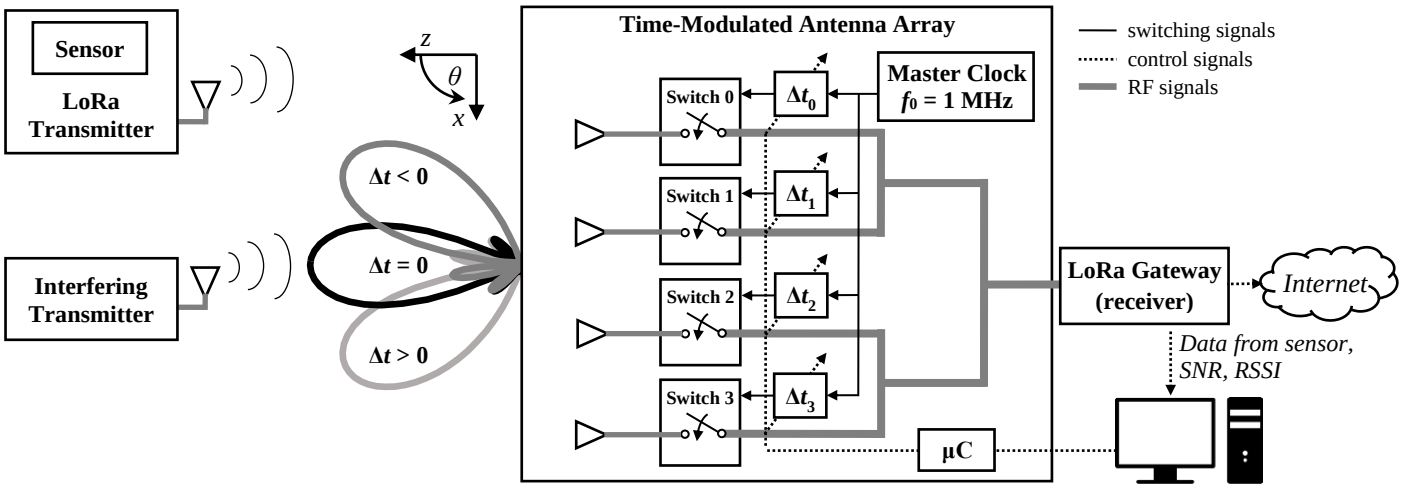

Fig. 1. Concept of TMAA for adaptive reception in LPWAN network.

$T_0 = 1/f_0$ and $f_c \gg f_0$ then it can be expressed in terms of the Fourier coefficients $M^{(k)}_n$. Thus (1) can be formulated as:

$$AF(\theta) = \sum_{k=-\infty}^{+\infty} e^{j2\pi(f_c+kf_0)t} \sum_{n=0}^{N-1} I_n M_n^{(k)} e^{j\beta nd\sin\theta} \qquad (2)$$

where $M^{(k)}_n$ is the kth complex Fourier coefficient of the nth modulating function and $k \in \mathbb{Z}$. According to (1) and (2) the periodic time-variation results in generation of sidebands [14]. Sidebands can be considered as partial patterns of the TMAA and used for the beam-steering [15]. This property enables application of TMAAs in adaptive wireless systems to improve the link budget in the desired direction while suppressing interfering signals approaching from other directions.

B. TMAA Gain and Efficiency

The realized gain of the TMAA can be expressed as:

$$G_R^{(k)} = D_0 \eta_r \eta_f \eta_{\text{mod}}^{(k)} \qquad (3)$$

where D_0 is the directivity of the non-modulated array, η_r is the radiation efficiency of the non-modulated array, η_f is the efficiency of the feeding network with switches in the static mode, and $\eta^{(k)}_{\text{mod}}$ is the time modulation efficiency when only the kth component is utilized [9]. If the TMAA is based on SPST switches and the switch-on duration equals $T_0/2$, then $\eta^{(-1)}_{\text{mod}}$ = 10.13%. This relatively low time modulation efficiency can be compensated with high directivity. For the broadside linear array the peak directivity can be approximated with the following formula [16]:

$$D_0 = 2N\frac{d}{\lambda} \qquad (4)$$

According to (3) and (4), the linear TMAA with SPST switches should be composed of at least 10 elements in order to compensate for the power losses caused by the time modulation and match the gain of a single non-modulated antenna.

In a general sense the directivity of N-element linear array is a function of the angle θ and depends on the phase progression $\Delta\phi$. It can be approximated with the following formula [16]:

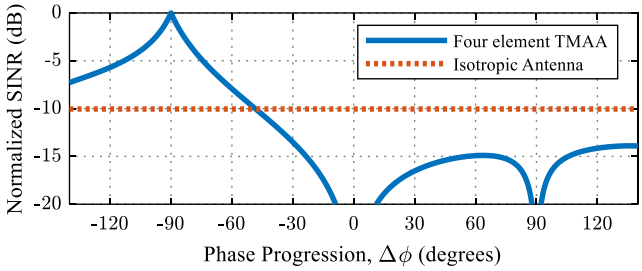

Fig. 2. Comparison of SINR obtained with four element TMAA and isotropic antenna.

$$D(\theta) = D_0 \frac{\sin\left(\frac{N}{2}\beta d\sin(\theta) + \Delta\phi\right)}{\frac{N}{2}(\beta d\sin(\theta) + \Delta\phi)} \qquad (5)$$

Control of the phase progression enables the beam-steering which can be used for adaptive signal reception.

C. Signal-to-interference-plus-noise ratio

The power of sidebands inherently generated by the TMAA for the desired and interfering signal can be calculated as $S^{(k)} = P_s G_R^{(k)}(\theta_s)/L_s$ and $I^{(k)} = P_i G_R^{(k)}(\theta_i)/L_i$, respectively, where P is the transmitted power, θ is the angle of arrival, L is the propagation loss, and the subscripts 's' and 'i' refer to the desired and interfering signals, respectively. The signal-to-interference-plus-noise ratio (SINR) can be calculated as $SINR^{(k)} = S^{(k)}/(I^{(k)} + N)$, where N is the total noise power. Fig. 2 shows comparison of the normalized SINR in the receiver which utilizes the first negative sideband component ($k = -1$) generated by the 4-element TMAA and an isotropic antenna for a specific case when $L_s = L_i$, $\theta_s = 30°$, $\theta_i = 0°$, $P_i = 10P_s$ and $N = 0.1P_s$. When $\Delta\phi = -90°$ then the null of the radiation pattern is directed toward the interfering transmitter, and the main beam is directed toward the desired transmitter. Because the time modulation efficiency applies equally to the power of desired and interfering signals, it has no impact on the ratio between both values, therefore the SINR obtained for a single sideband component can be significantly higher compared to the reception with the isotropic antenna.

III. System Design

A. LoRa Devices

Fig. 1 shows a LPWAN network based on the LoRa technology. It consists of the LoRa transmitter with a sensor, the interfering transmitter, the TMAA used in the receive mode, and the receiving LoRa gateway. Both the LoRa transmitter and the receiving LoRa gateway were based on a commercially available wireless transceiver RF-LoRa-868-SO [17]. This transceiver is based on SX1272 integrated circuit which provides two fundamental quality indicators, i.e. the received signal strength indicator (RSSI) and the signal-to-noise ratio (SNR), where the noise power includes also distortion and interference. Both LoRa devices were configured to transmit or receive signals with the spreading factor of 12, the code rate of 4/5 and the channel bandwidth of 250 kHz.

B. Design of the TMAA

The designed TMAA after fabrication is presented in Fig. 3. It consists of four reflector-backed dipoles arranged into a linear array. The spacing between dipoles equals 17.5 cm which corresponds to the half of the wavelength in the free space at the operational frequency. Each element of the array is connected to a throw of the single-pole double-throw (SPDT) radio frequency (RF) switch. Another throw of each switch is terminated to 50 Ω in order to realize the time modulation by means of the on/off switching. A commercially available switch SKY13286-359LF was selected due to a relatively short RF rise/fall time (30 ns), low insertion loss at 868 MHz (0.8 dB), and high isolation between switching ports (62 dB) [18].

The control unit of the TMAA is composed of a master clock generator and four daisy-chained programmable delay lines (PDLs). The master clock generator is based on Si5351A integrated circuit, which generates four synchronized clock signals with the duty cycle of 50%, hence the on-state and the off-state durations for all elements are equal to the half of the modulation period, i.e. 500 ns each. PDLs are utilized to apply delays to each of these clock signals. The maximum delay is 1 275 ns and it can be controlled with a step of 5 ns.

Fig. 4a shows normalized antenna patterns measured over the first negative partial pattern ($k = -1$) for different delay-progressions of the time modulation functions $\Delta t = \Delta t_n - \Delta t_{n-1}$ which translates to the phase progression introduced to the sideband components: $M_n^{(k)} = M_0^{(k)} e^{-j2\pi kn\Delta t/T_0}$ [19]. The measured 3 dB scanning range covers a wide sector of 95° because of the almost omnidirectional element pattern. Fig. 4b shows the main beam and nulls for three representative values of the delay-progression. In total 171 different TMAA patterns for Δt varying from –425 ns to 425 ns were measured. Obtained directions of the main beam and four nulls versus the delay-progression are presented in Fig. 5 which demonstrates, that the beam-steering is achieved jointly with the null-steering. Independent and more flexible formation of nulls is possible; however, it would require advanced synthesis of the TMAA pattern or implementation of an adaptive algorithm which is out of the scope of this letter.

Fig. 3. Antenna array composed of four dipoles with metallic reflectors.

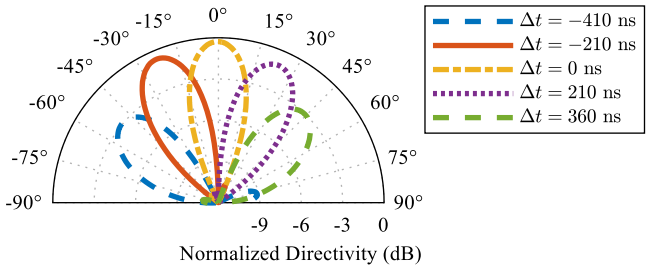

(a)

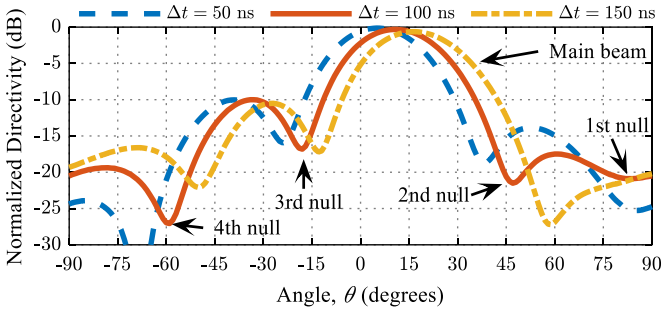

(b)

Fig. 4. Antenna patterns measured over the first negative sideband component ($k = -1$) for different values of delay progression Δt: (a) polar coordinates, (b) rectangular coordinates.

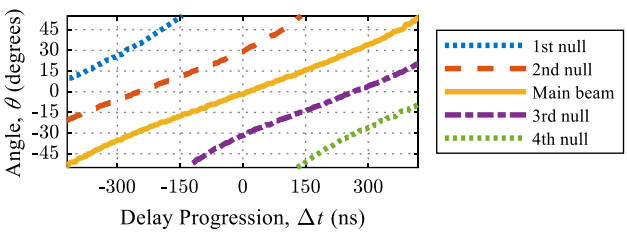

Fig. 5 Direction of main beam and nulls measured over the first negative sideband pattern ($k = -1$) for different values of delay progression Δt.

IV. Experimental Study Of LoRa Receiver with TMAA

A. Experimental Setup

The experimental setup was constructed inside an anechoic chamber according to a diagram presented in Fig. 1. Both LoRa devices used in the experiment (the transmitter with a sensor and the receiving gateway) were designed according to the description given in the Section II-A. The interfering transmitter was realized by using the Rohde & Schwarz SMBV100A signal generator transmitting a narrow-band signal at frequency 869 MHz via a standard gain antenna. The setup was arranged in an unfavorable way, i.e. the interfering transmitter was located in front of the receiving antenna (TMAA), whereas the desired LoRa transmitter was located at the angle of –30°.

B. System Configuration

The designed TMAA was applied to the LoRa gateway as a receiving antenna. The LoRa transmitter was configured to transmit at the carrier frequency f_c = 869 MHz in a narrow bandwidth of 250 kHz. The master clock of the TMAA was set to f_0 = 1 MHz to avoid aliasing between spectral replicas of the received signal. Fig. 6 shows two spectra of the original signal received with a conventional antenna and the time-modulated signal received with the TMAA. In the latter case, in result of the periodic switching, the spectrum is composed of spectral replicas located at $f_c + kf_0$. In order to take advantage of an additional TMAA capability (i.e. beam-steering) the LoRa gateway was tuned to process the first negative spectral replica located at $f_c - f_0$ = 868 MHz. The power level of this component is 10 dB lower compared to the original signal which means that the TMAA-based beam-steering introduces a substantial loss of the received signal power.

C. Interference Suppression

The performance of the interference suppression obtained by means of the beam-steering was investigated experimentally. The output power of the LoRa transmitter was fixed, whereas the output power of the interfering transmitter (P_i) has been changing in a range from –30 dBm to –10 dBm. The TMAA was operating in a scanning mode, i.e. the delay progression has been incrementally changed from –425 ns to 425 ns with a step of 5 ns in order to obtain a continuous change of the main beam and nulls locations according to Fig. 6. The values of the RSSI and the SNR reported by the receiver of the LoRa gateway are presented in Fig. 7 and Fig. 8, respectively. Measurements were repeated 10 times and averaged to decrease the quantization error.

For Δt = 0 the first negative partial pattern of the TMAA is configured for a broadside reception. In consequence, due to an unfavorable spatial arrangement, the main beam is directed toward the unwanted transmitter (0°) and the third null is directed toward the LoRa transmitter (–30°) which causes a substantial drop of both the RSSI and the SNR.

For Δt < –100 ns the main beam is directed toward the LoRa transmitter which has a positive impact on the quality of transmission. For example, peak values of the RSSI and the SNR were obtained for Δt = –275 ns. A high SNR is achievable also, if the main beam is not directed toward the LoRa transmitter. For example, if Δt = 120 ns then the signal from LoRa transmitter is received by a sidelobe. Although, in such a case, its value is more susceptible to the power of the interfering signal. A significant change of the SNR is observed when Δt is in a range between 200 ns and 300 ns, because the third null and the fourth null pass the direction of the interfering transmitter and the direction of the LoRa transmitter, respectively. After comparing all configurations of the TMAA we can summarize that the best improvement of the SNR was observed for a case of a strong interference (P_i = –10 dBm). In such a case the SNR was improved by 25 dB compared to a broadside configuration of the TMAA.

D. Discussion of Results

Both the RSSI and the SNR depend substantially on the shape of the antenna pattern, which is controlled by Δt. The RSSI reported by the LoRa receiver gives a coarse information of the received signal strength. Its variation over Δt is similar for different P_i which indicates immunity of this parameter to the interference; however, its influence is still noticeable. For example, the highest RSSI was reported for a strong interference (P_i = –10 dBm). Hence, calculation of RSSI also includes some part of the interfering signal and should not be considered as a figure of merit. The SNR is very sensitive to an interference. Its top values were obtained when the main beam was directed toward the LoRa transmitter and the second null was directed toward the interfering transmitter.

V. Conclusion

We have presented the interoperability between the TMAA and a commercial of-the-shelf LoRa transceiver and demonstrated that the beam-steering obtained over the sideband components is suitable for implementation in LPWAN receivers. The experimental results proved that the beam-steering can be effectively utilized to improve the RSSI and SNR even in the presence of an interference. The feasibility of an adaptive LoRa receiver based on the TMAA was verified without an adaptive algorithm; however, the proposed design demonstrates a potential for a future work dedicated to adaptive optimization of the antenna pattern in dynamically changing conditions.

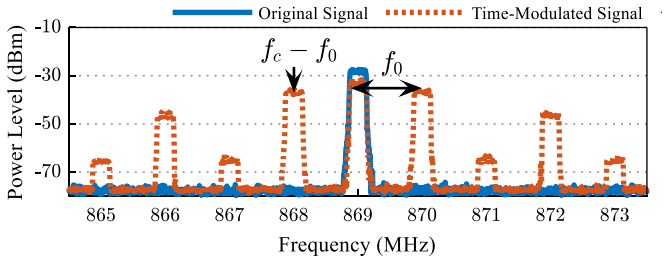

Fig. 6. Spectra of original and time-modulated signals measured with spectrum analyzer in max hold mode.

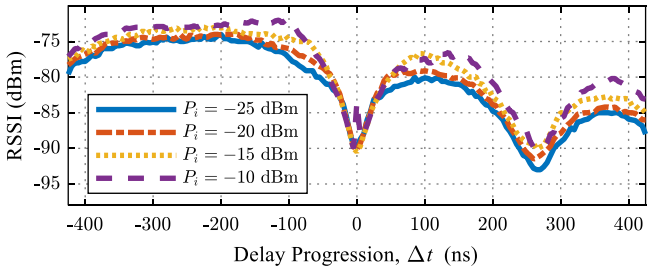

Fig. 7. RSSI measured for different power of interfering signal.

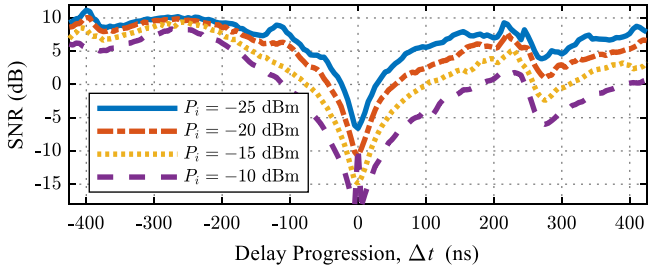

Fig. 8. SNR measured for different power of interfering signal.

REFERENCES

[1] A. Ikpehai *et al*., "Low-Power Wide Area Network Technologies for Internet-of-Things: A Comparative Review," in *IEEE Internet of Things Journal*, vol. 6, no. 2, pp. 2225-2240, April 2019.

[2] *ERC Recommendation 70-03 Relating to the use of Short Range Devices (SRD)*, Electronic Communications Committee, 1997, Accessed: Feb. 19, 2020. [Online]. Available: https://www.ecodocdb.dk/download/25c41779-cd6e/Rec7003e.pdf

[3] K. Staniec, M. Kowal, "LoRa performance under variable interference and heavy-multipath conditions", *Wireless Communications and Mobile Computing*, vol. 2018, pp. 1-9, 2018.

[4] A. Augustin, J. Yi, T. Clausen, W.M. Townsley, "A Study of LoRa: Long Range & Low Power Networks for the Internet of Things," Sensors, vol. 16, no. 9, 1466, 2016

[5] B. Reynders and S. Pollin, "Chirp spread spectrum as a modulation technique for long range communication," *23rd IEE Symp. Commun. Vehicular Techn. (SCVT)*, Mons, Belgium, Nov. 2016, pp. 1-5

[6] A. Alexiou and M. Haardt, "Smart antenna technologies for future wireless systems: trends and challenges," in *IEEE Communications Magazine*, vol. 42, no. 9, pp. 90-97, Sept. 2004.

[7] P. Rocca, G. Oliveri, R. J. Mailloux, and A. Massa, "Unconventional Phased Array Architectures and Design Methodologies - A Review," *Proc. IEEE*, vol. 104, no. 3, pp. 544–560, May 2016.

[8] R. Maneiro-Catoira and J. C. Bregains and J. A. Garcia-Naya and L. Castedo, "On the Feasibility of Time-Modulated Arrays for Digital Linear Modulations: A Theoretical Analysis," *IEEE Tran. Antennas Propag.* , vol. 62, no. 12, pp. 6114–6122, 2014.

[9] Q. Chen, J. Zhang, W. Wu, and D. Fang, "Enhanced Single-Sideband Time-Modulated Phased Array with Lower Sideband Level and Loss," *IEEE Trans. Antennas Propag*, vol. 68, no. 1, pp. 275–286, 2020.

[10] R. Maneiro-Catoira, J. Bregains, J. A. Garcia-Naya, and L. Castedo, "Time-Modulated Phased Array Controlled With Nonideal Bipolar Squared Periodic Sequences," *IEEE Antennas Wireless Propag. Letters*, vol. 18, no. 2, pp. 407–411, 2019.

[11] G. Bogdan and Y. Yashchyshyn, "Experimental study of signal reception by means of time-modulated antenna array," in *21st Int. Conf. Microw. Radar Wireless Commun. (MIKON)* , Kraków, Poland, 2016, pp. 1–4.

[12] G. Bogdan, K. Godziszewski, Y. Yashchyshyn, C. H. Kim, S. Hyun, "Time Modulated Antenna Array for Real-Time Adaptive Beamforming in Wideband Wireless Systems—Part I: Design and Characterization", *IEEE Trans. Antennas Propag.*, 2019 [Online]. Available: https://ieeexplore.ieee.org/document/8657780

[13] R. Maneiro-Catoira, J. Bregains, J. A. Garcia-Naya, and L. Castedo, "Time modulated arrays: from their origin to their utilization in wireless communication systems," Sensors, vol. 17, no. 3, p. 590, Mar. 2017

[14] J. C. Bregains, J. Fondevila-Gomez, G. Franceschetti, and F. Ares, "Signal Radiation and Power Losses of Time-Modulated Arrays," in *IEEE Tran. Antennas Propag*, vol. 56, no. 6, pp. 1799-1804, June 2008.

[15] L. Poli, P. Rocca, G. Oliveri, and A. Massa, "Harmonic Beamforming in Time-Modulated Linear Arrays," *IEEE Tran. Antennas Propag*, vol. 59, no. 7, pp. 2538–2545, 2011.

[16] C. A. Balanis, Antenna theory: analysis and design. Hoboken, New Jersey: John Wiley & Sons, 2012.

[17] RF SOLUTIONS, *RF-LoRa LongRange Transceiver*. (2018). Accessed: Jun. 9, 2020. [Online]. Available: https://www. rfsolutions.co.uk/downloads/1538123141DS-RFLoRa-7.pdf

[18] Skyworks Solutions, *Data Sheet SKY13286-359LF: 0.1 to 6.0 GHz High Isolation SPDT Absorptive Switch*. (2017). Accessed: Jun. 9, 2020. [Online]. Available: https://www.skyworksinc.com/-/media/SkyWorks/Documents/Products/101-200/SKY13286_359LF_200570K.pdf

[19] G. Bogdan, Y. Yashchyshyn, and M. Jarzynka, "Time-Modulated Antenna Array with Lossless Switching Network*," IEEE Antennas Wireless Propag. Letters* , vol. 15, pp. 1827–1830, 2016.